sustainability

MDPI

Article

Construction Solutions and Materials to Optimize the Energy Performances of EPS-RC Precast Bearing Walls

Albina Scioti, Mariella De Fino *, Silvia Martiradonna and Fabio Fatiguso

DICATECh Department, Polytechnic of Bari, Via Orabona, 4, 70125 Bari, Italy; albina.scioti@poliba.it (A.S.); silvia.martiradonna@poliba.it (S.M.); fabio.fatiguso@poliba.it (F.F.)

* Correspondence: mariella.defino@poliba.it

Abstract: The design and employment of envelope components showing high thermal performances for new buildings and deep renovations must take into account the overall impact of the production process in terms of environmental sustainability. To this end, precast construction solutions and secondary raw materials provide added value to the energy quality of building products. With regard to the abovementioned issues, the paper is focused on the performance optimization of expanded polystyrene-reinforced concrete (EPS-RC) precast bearing walls, already developed and patented within a previous research project entitled "HPWalls. High Performance Wall Systems", and herein improved according to two complementary requirements: on the one hand, the addition of recycled EPS particles to the concrete mixtures and, thus, the assessment by lab tests of the correlation between the thermal and mechanical properties for several mix-design specimens; on the other hand, a study using analytical simulations of the most suitable joint solutions among modular panels in order to prevent thermal bridges. The achieved results validate the proposed optimization strategies and provide reliable data for market applications in the building sector.

Keywords: precast walls; energy performances; recycled EPS; thermal bridge correction

check for updates

Citation: Scioti, A.; De Fino, M.; Martiradonna, S.; Fatiguso, F. Construction Solutions and Materials to Optimize the Energy Performances of EPS-RC Precast Bearing Walls. *Sustainability* **2022**, *14*, 3558. https://doi.org/10.3390/su14063558

Academic Editors: Marta Maria Sesana, Graziano Salvalai and Roberto Lollini

Received: 20 February 2022
Accepted: 15 March 2022
Published: 17 March 2022

1. Introduction

Over the past decades, energy consumption has dramatically increased in the building sector, which is currently responsible for about 40% of the total primary energy use in the US and EU. Consequently, energy efficiency through properly designed, constructed and operated buildings, according to the Net Zero Energy Buildings vision, has become paramount to cope with energy shortages, carbon emissions and their serious threats to our living environment [1], especially because the enduring climate change is expected to increase the global energy demand in the long term [2]. In this regard, along with new constructions, a leading role should be played by the existing building stock, particularly the residential buildings, whose deep renovation is a major challenge in terms of energy efficiency and self-sufficiency [3]. To this end, the main strategy concerns the decrease of the operational energy consumption, recognized as the main feature of energy efficient buildings and addressed by the performance improvement of envelope components and the exploitation of renewable sources. However, the environmental impact of the construction and demolition phases through the suitable selection of building products should also be taken into account, especially if the abovementioned performance improvement requires the employment of a larger number of materials [4–6].

Within this framework, a relevant contribution might be provided by precast building components. In fact, while conventional cast-in-place techniques generally lead to many concerns such as low field productivity, unreliable quality, high resource and energy consumption, frequent safety accidents and significant pollution, the standardization of the design, prefabrication of structural elements and mechanization of on-site construction techniques are acknowledged as valuable requirements for the economic, social and environmental sustainability of the building sector, both for new constructions and retrofitting [7–10]. In addition, the energy optimization of precast building components has been addressed by several authors, as will be detailed in the following section, in terms of the selection of sustainable materials and the development of high-performing insulation solutions, according to life-cycle and circular economy approaches. All of the abovementioned issues are particularly relevant for vertical envelope components, which cover the largest area of the external building surface and act as the main frontier between the outdoor environment and the indoor space.

With reference to the outlined topics, the paper will focus on precast reinforced concrete (RC) walls for new constructions and the deep renovation of the residential building stock, by presenting the most current state-of-the-art technologies, as well as some studies focused on improving energy performance by employing innovative, natural and recycled materials and through the optimization of the constructional layout for the correction of thermal bridges (Section 2). Thus, starting from the design of an expanded polystyrene-reinforced concrete (EPS-RC) wall system (Section 3.1), as patented by the authors previously (Italian patent N. 0001429016, registered on 30 June 2017), further developments are proposed and discussed (Section 3.2) that relate to the exploitation of recycled EPS in the concrete mixtures (Section 4.1) and the design of the construction joints among wall modules to prevent thermal bridges (Section 4.2).

2. State-of-the-Art

Several solutions were developed and tested for achieving reliable and efficient precast vertical systems with thermal performances that could make them suitable for the residential, office and commercial sectors and their relative normative energy requirements. In particular, three solutions, based on the combination of RC and EPS, were widely studied:

- Precast concrete sandwich panels (PCSPs), which are composite cladding types encompassing concrete wythes that embed a layer of thermal insulation. They are fully fabricated in the factory, thus ensuring greater quality control and a reduced risk of poor detailing, in addition to further performances including fire resistance, durability and thermal insulation [11–14];
- EPS-based formwork blocks (EPSFBs), consisting of modular interlocking EPS building blocks as permanent formwork for the construction of in-situ concrete walls, both bearing and non-bearing, with high thermal, acoustic and fire resistance performances [15,16].
- Insulated concrete form walls (ICFWs), made of rigid plastic (e.g., EPS), are foam walls that hold concrete together during the curing operation and remain in place permanently afterwards to serve as thermal insulators [17,18].

With a specific focus on the energy behavior of the abovementioned systems, particularly the best-established one, i.e., PCSPs, several research works recently addressed the improvement of their performances based on different and complementary strategies: on the one hand, the employment of high-performing products, and on the other hand, the optimization of the constructional layout.

Concerning the employment of high-performing products, some cutting-edge artificial materials were proposed, such as phase change materials (PCMs) to maximize the ability to store heat and slow down the rate of heat transfer [19,20], and vacuum insulation panels (VIPs), viewed as a viable solution for the space-saving attributes of high-performance walls [21]. Alternatively, natural products were used and tested. Wood bio-concretes (WBCs), namely cement-based materials with complete or partial substitution of mineral aggregates by wood particles, can offer an attractive solution for the low-cost transport of vegetable resources to the industries [22]. Similarly, the replacement of polymer-based insulation with high porosity hemp composites was proposed and validated by laboratory tests, along with the assessment of the amount of carbon dioxide emissions saved during the production phase by replacing traditional insulation with bio-based materials [23]. Moreover, in several cases, waste products were added to the manufacturing of the concrete mixture, including: co-fired blended ash (CBA), an industrial by-product where coal, agricultural residues and wood pellets are co-fired in boilers for heat generation [24]; wood bio-mass ash (WBA) from power plants [25]; food industry-filtered recycled diatoms from the production of beer and wine [26]; and recycled EPS, as a replacement of up to 50% of the concrete aggregate for obtaining lightweight panels with optimized embodied energy [27–29]. The latter approach is particularly inspiring when taking into account that the waste products are generally available in the same factory.

Concerning the optimization of the constructional layout, some authors focused on the stratigraphic configuration of the panels. For instance, a study [30] concerned the development of precast concrete three-wythe sandwich wall panels with potential improved thermal performances. The system has three concrete wythes and two insulation layers, and all three concrete wythes are connected by solid concrete regions, so that the connections between successive concrete wythes are staggered in location and the total thermal path length through the concrete is extended. Furthermore, other authors focused on the design of the connectors that join the insulation and the concrete layers, creating a thermal bridge, the extent of which depends on the size and material of the connector. For this purpose, steel connectors wrapped with grooved nylon [31] and different shaped steel connectors were studied in order to minimize the problem [32].

Within the state-of-the-art on EPS-RC precast bearing walls for the residential sector, a specific system [33,34] was designed, realized and tested by the authors within a closed research project entitled "HPWalls. High Performance Wall Systems", funded by the European Regional Development Fund (ERDF) of the Puglia Region (south Italy), in cooperation with a local company. The company specializes in the production of so-called precast concrete double skin shear walls (PCDSSWs), which have two identical precast reinforced concrete panels, connected by truss-type reinforcements and completed as a monolithic wall by onsite casting concrete in the middle region enclosed by the two panels [35,36]. Taking into account that the same company also has a production chain for EPS-based flooring components, such as predalles slabs, for the civil and tertiary sector, the HPWalls system was meant to make the PCDSSWs suitable for residential buildings by providing the necessary thermal insulation by EPS. Compared to the abovementioned three EPS-RC solutions, the idea was to maximize the advantages and minimize the disadvantages of the alternatives [37–40]. Thus, the relative lightness and ease of transport of semi precast components and the thermal protection of the whole RC wall by the outer insulation layer were retained, differently from PCSPs. Moreover, the availability of timesaving big-sized panels was preferred over EPSFBs and the support of concrete form panels to hold the onsite concrete pouring and curing, an alternative of EPS form panels in ICFWs.

The result, which has been protected by a national patent since 2017 ("Prefabricated wall with high mechanical, thermo-hygrometric and acoustic performance for non-load-bearing and load-bearing walls". Designated inventors: Luigi Amati, Albina Scioti, Giambattista De Tommasi, Fatiguso Fabio, Alessandra Fiore), is a multi-layered wall, based on the off-site employment of external EPS formwork panels, hosting reinforced concrete panels on the internal sides. The RC panels are mutually connected by transversal truss reinforcement, placed in the inner cavity, which later hosts the onsite concrete casting. Moreover, the wall does not require steel connectors crossing the insulation panels, which are coupled to the precast concrete panels during the factory production chain.

Following the innovative approach of the basic layout of the patented wall, the present study aims to improve the overall energy performance of the system, following the complementary strategies acknowledged by the scientific community, as previously discussed. In detail, the employment of high-performing products will herein refer to the addition of recycled EPS particles to the concrete mixtures, that was proven to be an interesting research field by several recent studies in order to improve the lightness, insulation and carbon footprint of the conglomerate [41,42]. For this purpose, some lab tests aimed at assessing the correlation between thermal and mechanical properties for several mix-design specimens will be discussed, where the sand was partially or totally replaced in volume for the entire granulometric curve or for selective grain sizes.

Moreover, the optimization of the constructional layout will be pursued by the selection of the most suitable joint solutions among the modular panels, which is a key aspect not only for the structural stability [43,44], but also to prevent thermal bridges. The challenges associated with preventing air leaks between contiguous insulation modules on the external surface of the building envelope have been posed by several authors, particularly for the emerging technology of VIPs in external thermal insulation composite systems (ETICS). In fact, it was found that the panels undergo a thermal bridging effect at the edges of the modules as a result of the physical and geometrical properties, where the joint gap has great influence. The proposed solutions range from the application of sealing products to the use of EPS as an edge material [45,46]. The same problem applies to sandwich panels and metal panel wall systems, where an inner EPS core provides thermal insulation. Here, the most common solutions are related to the shaping of the interface between two modules, including S-shaped and tongue-and-groove layouts, in order to avoid a flat connection profile [47,48]. Nevertheless, the same principle is applied for commercial EPSFBs [15,16] with vertical and staggered protruding ribs.

In order to prevent thermal bridging effects at the connection between contiguous wall panels, some analytical simulations through 3D heat transfer analysis will be presented [49,50], focused on the shaping of the joints in analogy to other EPS-based systems. The simulations will also help assess the potential thermal anomalies due to the wall reinforcement, whereas the connection between the insulation and concrete layers is not provided by metallic elements.

It is worth mentioning that the research is willing to provide useful outcomes for both the industry and academia. In fact, for the industry, it aims to propose a model for the low-cost conversion/expansion of a precast production chain from PCDSSWs to insulating PCDSSWs that are suitable for the residential sector; to validate an alternative approach from EPS waste disposal to recycled EPS exploitation and virgin EPS saving, eventually in the same industrial site; and to provide reliable data on the proposed optimization strategies for the improved competitiveness and market attractiveness of the wall system for the partner factory and similar factories. For academia, the research aims to test methods and tools for manufacturing lightweight concrete with recycled EPS for a targeted precast component, as well as proposing some insights into the need to carefully design the horizontal and vertical connections between wall modules and assessing the potential anomalies from the concrete reinforcement, in order to avoid thermal bridges.

3. Materials and Methods

3.1. Background

The HPWalls is a multi-layered vertical module (Figure 1), up to 2500 mm in length and height, with an overall thickness of 300 mm. It is composed of 50 mm thick external EPS formwork panels, hosting 50 mm thick RC panels on the internal sides. The RC panels are mutually connected by transversal truss reinforcements, placed in the 150 mm inner cavity. It is worth mentioning that the production chain in the factory was not changed compared to the manufacturing process for PCDSSWs, where the metallic removable formworks for concrete pouring were used to host the EPS stay-in-place ones (Figure 2).

In fact, after plotting onto the metallic formworks the contours for the double wall to be produced (phase 1) and placing the shuttering profiles accordingly (phase 2), all by means of robot plotters that transfer the outline of the elements from the CAD data, the EPS panel is positioned ("new" phase 2bis). Thus, the reinforcement of the concrete panel and the truss framework of the wall are installed manually (phase 3) and the concrete is poured and vibrated (phase 4), before lifting the half-wall for one-day storage (phase 5). After one day, the half-wall is overturned and placed on another half wall (phase 6), which is produced following only phases 1, 2, 2bis and 4 (Figure 3).

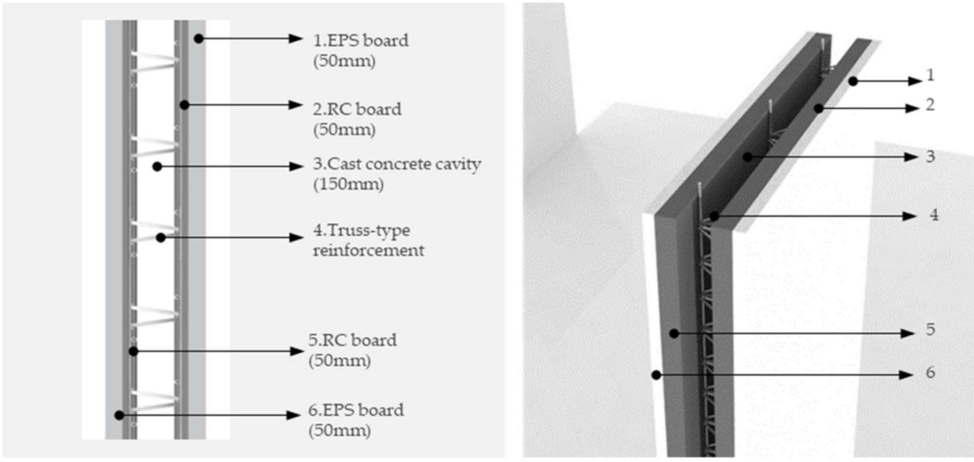

Figure 1. Layout of the "HPWalls" system.

Figure 2. Production chain of the "HPWalls" system, including phases 1 (**top left**), 3 (**top right**), 4 (**bottom left**) and 6 (**bottom right**).

The patented wall was conceived in order to meet the normative upper thresholds of thermal transmittance for vertical components, according to the Italian law DM 26/06/15.

In detail, considering the products already manufactured by the company, some specimens of EPS and concrete were tested in order to assess their hygrothermal properties. The experimental results, shown in Table 1, lead to the calculation of the wall thermal transmittance equal to 0.35 W/m^{2}K, as calculated in Table 2, assuming that the concrete increases its thermal conductivity of 40% when reinforced with 1% of steel, according to UNI EN ISO 10456:2008 [51]. It is worth mentioning that the thermal transmittance of the finished wall is further decreased depending on the specific design choices. For instance, an internal 20 mm layer of gypsum–lime plaster (conductivity equal to 0.26 W/mK) and an external 1 mm layer of acrylic plaster (conductivity equal to 0.31 W/mK) result in wall transmittance of 0.34 W/m^{2}K. Alternatively, the previous solution with internal 50 mm air cavity (resistance equal to 0.18 m^{2}K/W) for plant equipment and 50 mm plasterboard (conductivity equal to 0.21 W/mK) result in wall transmittance of 0.30 W/m^{2}K.

Figure 3. Prototype of "HPWalls" system.

Table 1. Measured hygrothermal properties of EPS and concrete for the basic layout of the patented wall.

Material	Density (kg/m^3)	TC [1] (W/mK)	TD [1] (10^{-6} m^2/s)	VHC [1] (106 J/m^3K)	WVP [1] (10^{-12} kg/(m s Pa))	WVRF [1] (-)
EPS_0	10	0.0391	1.180	0.033	7.03	27.5
C_0	2189.0	1.77	1.01	1.77	3.61	53.76

[1] TC = thermal conductivity; TD = thermal diffusivity; VHC = volumetric heat capacity; WVP = water vapor permeability; WVRF = water vapor resistance factor.

Table 2. Calculated thermal transmittance for the basic layout of the patented wall.

Layer	Thickness (m)	TC [1] (W/mK)	TR [1] (m^2K/W)
R_{SI} [2]			0.13
EPS_0	0.05	0.039	1.282
C_0	0.25	2.5	0.10
EPS_0	0.05	0.039	1.282
R_{SE} [2]			0.04
	WR [3] (m^2K/W)		2.83
	WT [3] (W/m^2K)		0.35

[1] TC = thermal conductivity; TR = thermal resistance; [2] R_{SI} = internal surface adductive resistance; R_{SE} = external surface adductive resistance; [3] WR = wall resistance; WT = wall transmittance (1/WR).

The hygrothermal performance of the building component to avoid critical surface humidity and interstitial condensation, according to UNI EN ISO 13788:2013 [52], was also successful. In detail, the calculation was run on a monthly basis, taking into account the climatic data for the city of Bari (south Italy) and the use as dwelling. Although critical conditions never occurred, the most unfavorable scenarios were found in winter (indoor: 20 °C, 65% RH; outdoor: 8.9 °C in February −14.2 °C in November; 73.3% RH in February, 79.2% RH in November).

3.2. Research Development

The improvement of the basic solution was addressed following two approaches.

The first approach concerned the replacement of the fine aggregate (sand) in the concrete mixtures with EPS granules, as discarded from the production process and crushed into a grinding machine in the same factory. The proposed solution is meant to optimize both the quality of the building component and the efficiency of the production process, taking into account that the EPS tailings, currently disposed of by the research partner company, would turn into a resource with beneficial effects on waste management and material exploitation, according to the principles of a circular economy.

In detail, based on similar experimental studies on lightweight EPS concrete, as previously mentioned [27–29,40,41] for precast and onsite structures, the replacement was designed, taking into account the size of the available recycled granules (96% in EPS volume ranging from 1 mm to 8 mm) and the mix design of the basic conglomerate as manufactured in the factory (64% in sand volume ranging from 1 mm to 8 mm). Thus, two methods were followed: on the one hand, substitution of increasing percentages of the volume of sand by EPS for the entire granulometric curve; on the other hand, substitution of the total volume of sand by EPS, previously graded by sieve analysis, for specific grain sizes. It is worth mentioning that the first method is documented as leading to lower mechanical performances, due to the overall differences in grain size distribution between sand and EPS. Nevertheless, it was still considered an alternative worthy of investigation, taking into account the potential advantages in terms of preparation time and resources for the factory operators.

All of the mixtures were tested in order to measure their thermal conductivity, thermal diffusivity and volumetric heat capacity by means of a portable device, the Isomet 2104 with a surface probe, supplied by Applied Precision Inc., according to UNI EN 12667:2002 [53]. Moreover, their water vapor permeability and water vapor resistance factor were assessed by the cup method, according to ISO 12572:2016 [54] in a Perani AC520 climate chamber (T = 23 °C; RU = 50%). Finally, the compressive strength was determined according to UNI EN 12390-2/3/4:2019 [55–57]. The final investigation involved classifying all of the mixtures as structural/non-structural and as lightweight/normal according to the Italian standards, and then assessing which one could offer the maximum performance solutions, namely the best thermal insulation for energy saving for load-bearing walls.

The second approach concerned the assessment of the geometry/shape of the panels, particularly their connection joints, in order to mitigate potential thermal bridges. The RC precast panels are generally installed by putting the modules side by side, leaving the function of making them cohesive to the onsite concrete casting. Thus, the interface might be responsible for construction thermal dispersions. The proposed optimization relied on the design of specific shaping of the vertical, horizontal and corner connection joints, followed by the finite element method (FEM) simulation of the heat flux and temperature distribution, in comparison with the basic layout. For this purpose, the software COMSOL Multiphysics® was implemented to carry out 2D and 3D simulations in the hypothesis of steady-state.

4. Results

4.1. Employment of Recycled EPS in Concrete Mixtures

The replacement of the fine aggregate (sand) in the concrete mixtures with EPS granules was carried out after the sieve selection of three sizes (1–2 mm, 2–4 mm, 4–8 mm). The concrete, which is commonly produced in the factory, was assumed as a reference specimen (S_0). Thus, several combinations were considered (Table 3), by substitution of increasing percentages in the volume of sand for the entire granulometric curve (S_1–S_4) and by selective substitution in the volume of sand with specific sizes (S_5–S_{10}).

In all cases, in order to increase the cohesion of the EPS granules with the binding agent (cement), the granules were preliminarily hydrophilized. Moreover, all of the mixtures were prepared with a water/cement ratio equal to 0.55 and the addition of a superplasticizer to improve the workability.

In order to measure the compression strength, $f_{ck,cube}$, three cubic specimens (150 × 150 × 150 mm) for each type were prepared and tested. The results are presented in Figures 4 and 5, with the latter showing how the compression strength decreases when the percentage in volume of the replaced sand increases. The values range from 39.96 MPa for S_7, corresponding to 83% of the reference specimen S_0 to 5.12 Mpa for S_4, corresponding to 11% of S0.

Furthermore, in order to measure the thermal properties, three cylindrical specimens (diameter = 100 mm, height = 50 mm) for each type were prepared and tested. The results are shown in Table 4, as well as in Figures 6 and 7, with the latter showing how the thermal conductivity decreases according to the density. Here, the thermal conductivity values range from 1.77 W/mK for S7, corresponding to 100% of the reference specimen S_0, to

0.45 W/mK for S_4, corresponding to 25% of S_0. For some specimens, the water vapor permeability and water vapor resistance factor were determined as well (Table 5).

Table 3. Characteristics of the EPS–concrete mixtures (background color highlights the granulometric composition of EPS and sand in the mixture).

<table>
<tr><th rowspan="3">Code</th><th colspan="6">EPS</th><th colspan="6">SAND</th></tr>
<tr><th colspan="6">Grain Size (mm)</th><th colspan="6">Grain Size (mm)</th></tr>
<tr><th>0–0.5</th><th>0.5–1</th><th>1–2</th><th>2–4</th><th>4–6</th><th>6–8</th><th>0–0.5</th><th>0.5–1</th><th>1–2</th><th>2–4</th><th>4–6</th><th>6–8</th></tr>
<tr><td>S_0</td><td colspan="6"></td><td colspan="6">100%V</td></tr>
<tr><td>S_1</td><td colspan="6">25%</td><td colspan="6">75%V</td></tr>
<tr><td>S_2</td><td colspan="6">50%</td><td colspan="6">50%V</td></tr>
<tr><td>S_3</td><td colspan="6">75%</td><td colspan="6">25%V</td></tr>
<tr><td>S_4</td><td colspan="6">100%</td><td colspan="6"></td></tr>
<tr><td>S_5</td><td></td><td></td><td>V(1–2)</td><td></td><td></td><td></td><td colspan="2">V(0–1)</td><td></td><td colspan="3">V(2–4)</td></tr>
<tr><td>S_6</td><td></td><td></td><td></td><td>V(2–4)</td><td></td><td></td><td colspan="3">V(0–2)</td><td></td><td colspan="2">V(4–8)</td></tr>
<tr><td>S_7</td><td></td><td></td><td></td><td></td><td colspan="2">V(4–8)</td><td colspan="4">V(0–4)</td><td></td><td></td></tr>
<tr><td>S_8</td><td></td><td></td><td colspan="2">V(1–4)</td><td></td><td></td><td colspan="2">V(0–1)</td><td></td><td></td><td colspan="2">V(4–8)</td></tr>
<tr><td>S_9</td><td></td><td></td><td></td><td colspan="3">V(2–8)</td><td colspan="3">V(0–2)</td><td></td><td></td><td></td></tr>
<tr><td>S_{10}</td><td></td><td></td><td colspan="4">V(1–8)</td><td colspan="2">V(0–1)</td><td></td><td></td><td></td><td></td></tr>
</table>

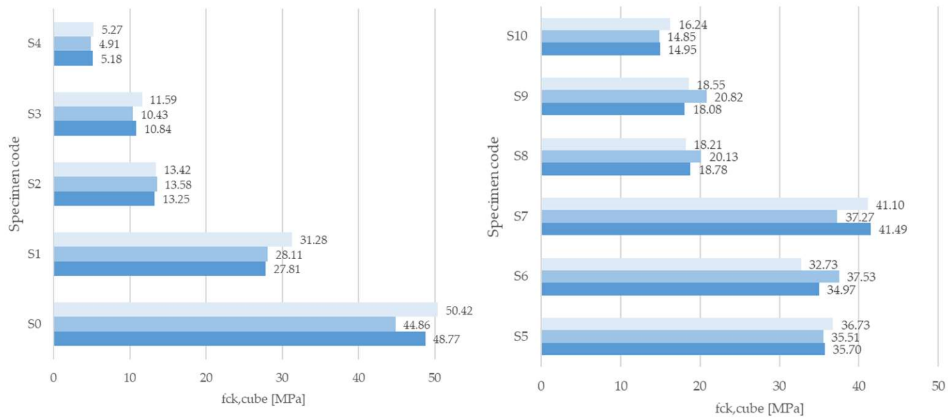

Figure 4. Mechanical strength of all of the tested specimens.

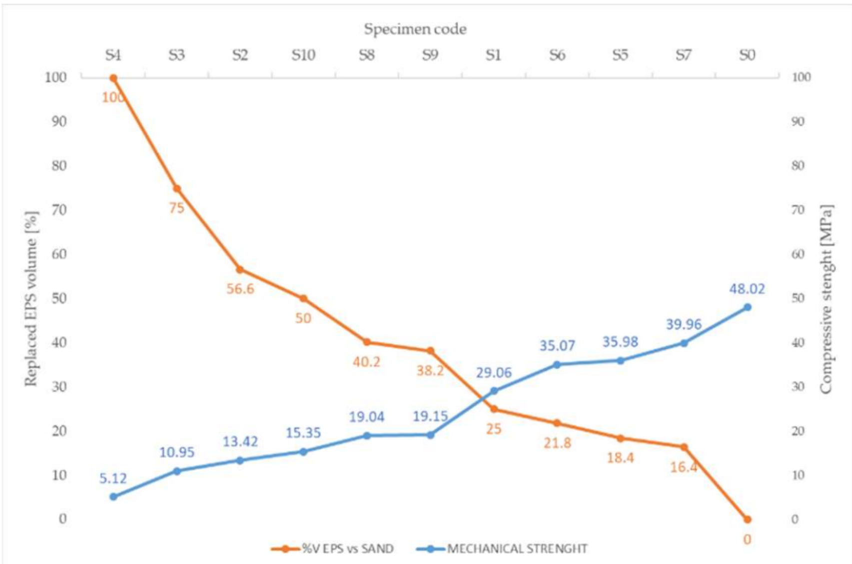

Figure 5. Average mechanical strength versus percentage in volume of replaced EPS.

Table 4. Measured thermal properties of the EPS–concrete mixtures.

Specimen Code	Density (kg/m^3)	TC [1] (W/mK)	TD [1] (10^{-6} m^2/s)	VHC [1] (106 J/m^3K)
S_0	2189.0	1.77	1.01	1.77
S_1	1974.9	1.35	0.83	1.63
S_2	1667.1	1.08	0.64	1.68
S_3	1377.3	0.84	0.56	1.52
S_4	1397.5	0.45	0.33	1.38
S_5	1973.31	1.42	0.87	1.64
S_6	2071.57	1.58	0.95	1.67
S_7	2147.27	1.77	1.02	1.73
S_8	1798.78	1.15	0.71	1.62
S_9	1892.38	1.28	0.80	1.60
S_{10}	1603.74	1.02	0.63	1.61

[1] TC = thermal conductivity; TD = thermal diffusivity; VHC = volumetric heat capacity.

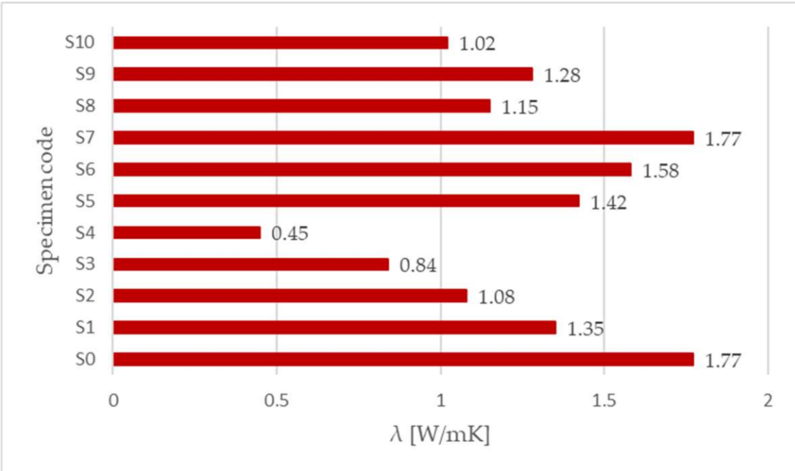

Figure 6. Thermal conductivity of the tested specimens.

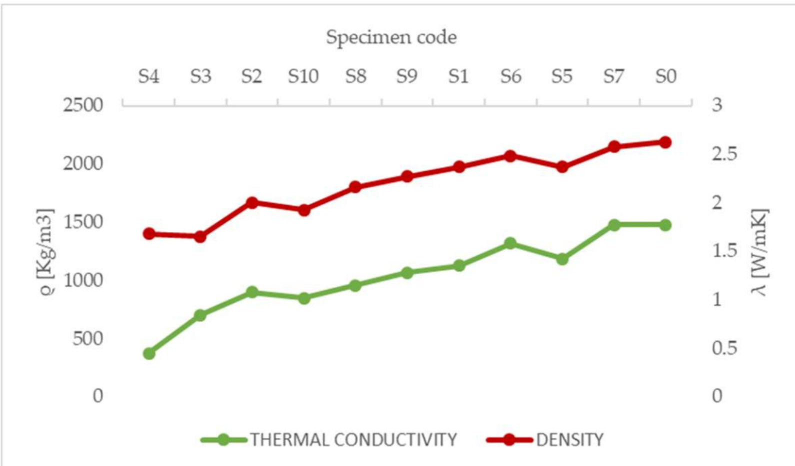

Figure 7. Thermal conductivity versus density.

Table 5. Measured hygrometric properties of the EPS–concrete mixtures.

Specimen Code	WVP [1] (10^{-12} kg/(m s Pa))	WVRF [1] (-)
S_0	3.61	53.76
S_1	4.65	41.59
S_2	4.57	42.46
S_3	7.58	26.45
S_4	6.60	29.29
S_5	7.34	26.29

[1] WVP = water vapor permeability; WVRF = water vapor resistance factor.

Based on the values of compression strength and density, the comparison against the thresholds provided by UNI EN 206:2021 [58] and NTC2018 [59] was performed in order to assess which mixtures might be considered lightweight concrete (1200 kg/m^3 $\leq \rho \leq$ 2000 kg/m^3) and structural concrete ($f_{ck,cube} \geq$ 18 MPa). Out of the ten specimens, three were not lightweight concrete. Out of the lightweight concrete specimens, four were suitable for structural purposes, while the remaining three were not (Table 6). In particular, it was confirmed that the substitution of increasing the percentages in the volume of sand by EPS for the entire granulometric curve (S_1, S_2, S_3, S_4), although more advantageous in terms of preparation time and resources for the factory operators, leads to a decrease in the density and mechanical properties, making the mixtures lightweight, but non-structural, except for S_1 with the lowest percentage (25%) of replacement.

Table 6. Classification of the tested specimens.

Specimen Code	Structural	Non-Structural	Lightweight	Normal
S_1	x		x	
S_2		x	x	
S_3		x	x	
S_4		x	x	
S_5	x			x
S_6	x			x
S_7	x			x
S_8	x		x	
S_9	x		x	
S_{10}		x	x	

Finally, the structural mixtures (S_1, S_5, S_6, S_7, S_8, S_9) were evaluated in terms of thermal conductivity, leading to the identification of S_8 (replacement of 1–4 mm sand with corresponding size EPS) as the maximum-performance solution, namely, the best heat insulation behavior (λ = 1.15 W/mK) for energy saving by a load-bearing wall.

4.2. Design of Construction Joints to Prevent Thermal Bridges

In order to prevent constructional bridges of the patented wall system, the horizontal and vertical joints were designed based on symmetrical S-shaped profiles for both the EPS and RC panels, so that the opposite profiles matched (Figure 8). Thus, a model of two panels with such connection joints was developed by CAD and imported into the software COMSOL Multiphysics® for 2D and 3D simulations of the thermal behavior in the hypothesis of steady-state, with the purpose of observing the temperature distribution and the heat fluxes in significant sections of the building component, given certain boundary conditions.

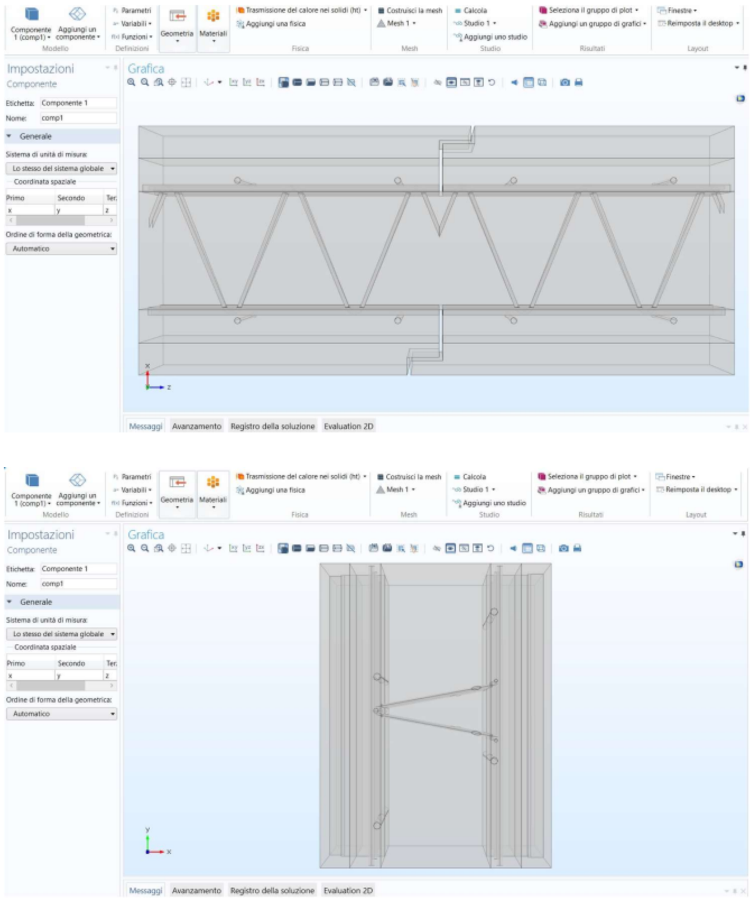

Figure 8. FEM-simulated wall.

As input data, the temperature difference between indoor and outdoor (Figure 9) was set equal to 20 °C (293.15 K) according to the Italian normative dispositions [60]. Moreover, the thickness, density, thermal conductivity and vapor permeability of the wall layers were attributed based on the experimental results of the previous section, considering that the external EPS and RC panels were made with the basic materials of the patented solution, while the inner cavity was composed of the structural mixture S_1, with a replacement of 25% of the sand with the equivalent volume of recycled EPS particles (Table 7).

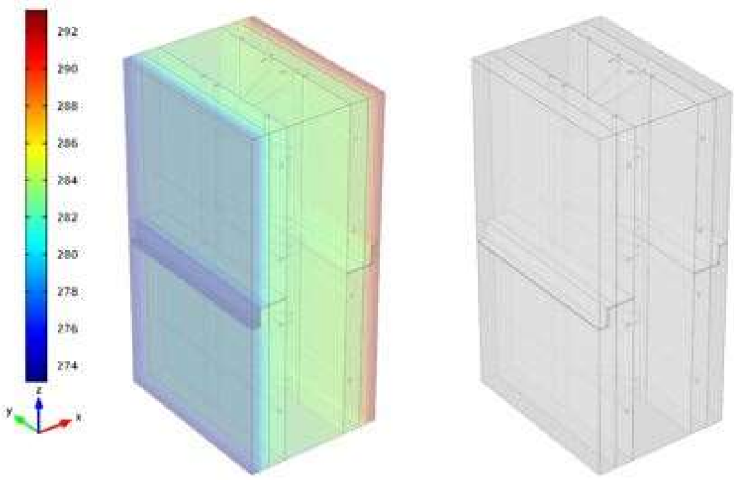

Figure 9. Temperature (K) set-up on the FEM wall.

Table 7. Properties of the FEM-simulated wall.

Wall Layer	Thickness (m)	Density (Kg/m^3)	TC [1] (W/mK)	WVRF [1] (-)
Indoor heat transfer coefficient			7.70	
EPS	50	10	0.04	27.5
S_0	50	2189	1.77	53.7
S_1	150	1975	1.35	41.6
S_0	50	2189	1.77	53.7
EPS	50	10	0.04	27.5
Outdoor heat transfer coefficient			25	

[1] TC = thermal conductivity; WVRF = water vapor resistance factor.

A preliminary analysis was meant to assess how the truss-type reinforcement in the inner cavity might affect the heat flux lines across the component. The results show that the thermal isometric lines undergo noticeable deviations across the metallic elements due to the variations of the local temperatures. Such deviations tend to lessen on the yz planes according to the distance from the inner cavity, and they are negligible on the external surface.

In detail, as shown in Figure 10, on the yz plane crossing the truss-type reinforcement, the thermal isometric lines are concentrated in limited areas where the temperatures significantly increase compared with the surroundings (right); on the yz plane crossing the RC panel, the lines become denser on the horizontal and vertical projections of the cavity reinforcement behind, although they correspond to lower temperature differences (central); on the yz plane crossing the EPS panel, they are marginally deviated in correspondence with the metallic elements (left). In this case, the temperature ranges from 273 K to 293 K (Figure 11). The results are confirmed by the temperature maps and heat flux lines on the xz and xy planes (Figure 12), where the local temperature differences across the reinforcement bars make the heat flux lines irregular and dense compared with the spaced and linear pattern in the precast panels.

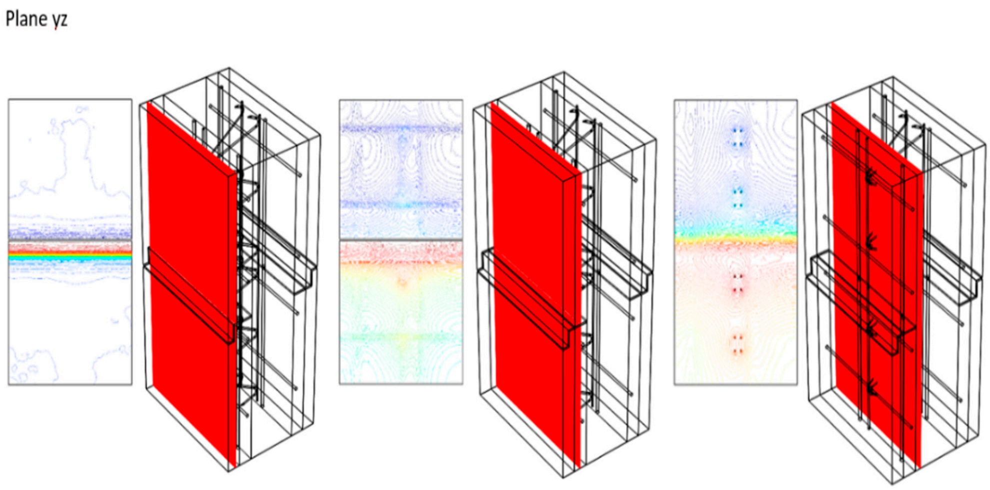

Figure 10. Overview of the thermal isometric lines on the yz planes.

Looking in more detail at the xy plane across the construction joints with the above-mentioned S-shaped profiles, the temperature distribution in the layers was observed. The results (Figure 13) point out how both the internal (50 mm) and the external (50 mm) EPS panels undergo a temperature drop of about 9 K each. Moreover, the temperature is almost stable across the S_1 inner cavity. Finally, both the internal (50 mm) and the external (50 mm) RC panels undergo a temperature drop of about 2 K each. It should be observed that no thermal anomalies resulted across the S-shaped profiles.

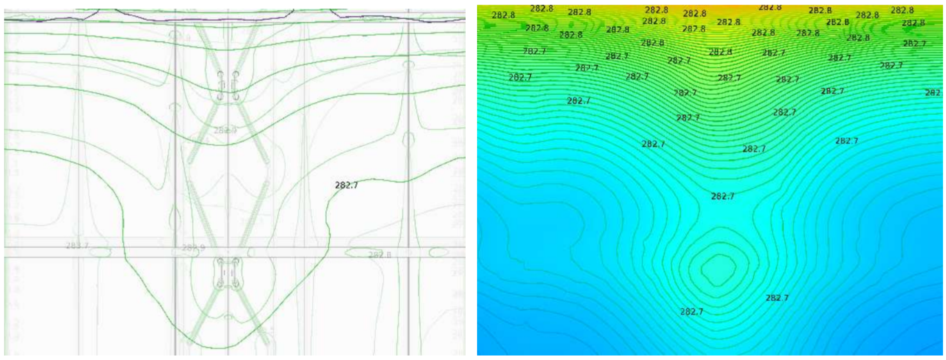

Figure 11. Detail of the thermal isometric lines on the panel with transparency on the reinforcement behind (**left**) and relative temperature map and values (**right**).

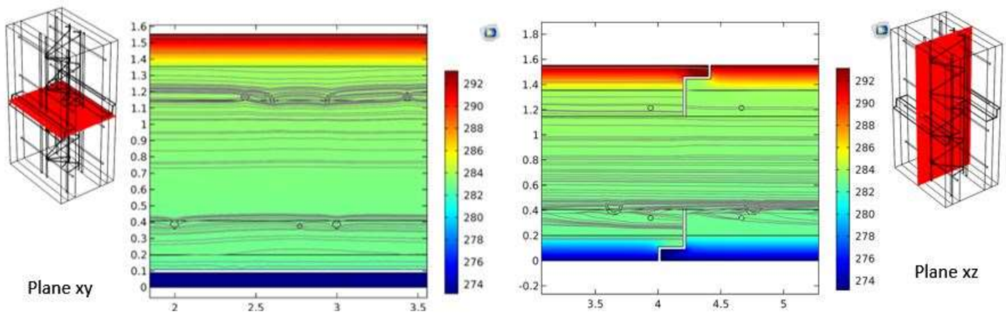

Figure 12. Temperature maps and heat flux lines on representative xz (**left**) and xy (**right**) plane.

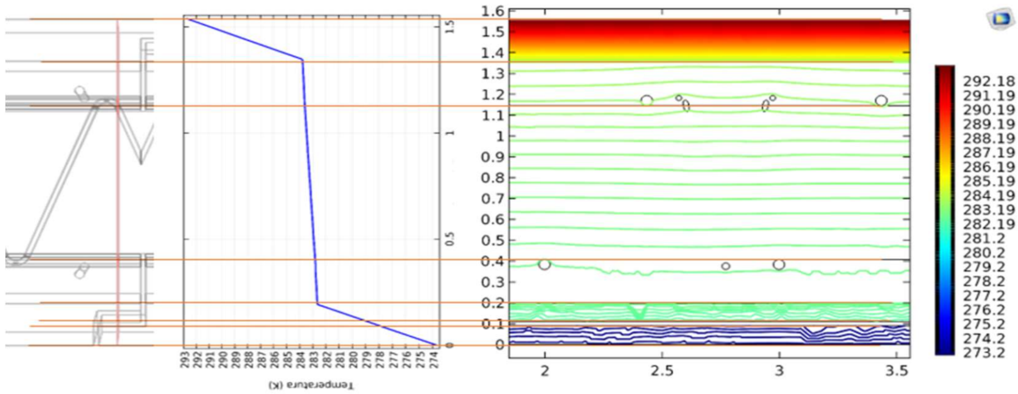

Figure 13. Temperature distribution (**left**) and isothermal lines on a representative xy plane (**right**) of the system with S-shaped joints.

The beneficial effects of the proposed connection joints were further validated by comparison with the conventional system, where the modules are installed side by side, leaving the function of making them cohesive to the onsite concrete casting. In this case (Figure 14), the temperature reductions from the indoor to the outdoor were found as follows: 1.5 K in the EPS panel, 3 K in the RC panel, 5 K in the inner cavity, 1 K in the RC panel and 9.5 K in the EPS panel. Therefore, looking at the thermal isometric lines for both solutions (Figure 15), it should be observed that the external EPS panel is always able to mitigate the thermal dispersions across the components. However, the solution with S-shaped profiles performs better in terms of temperature distribution. In fact, the temperature difference between the two EPS panels is about 1.5 K (282.5 K–284 K)—against about 8 K (284.5 K–292.5 K) in the conventional system—meaning that the inner cavity is kept warmer and more stable in terms of the thermal conditions across the transversal section. Furthermore, in the conventional system, a thermal bridge occurs at the joints, where the temperature trend is perturbed and the thermal isometric lines are arranged according to the typical "bottleneck" layout due to physical discontinuities with concentric and opposite curves.

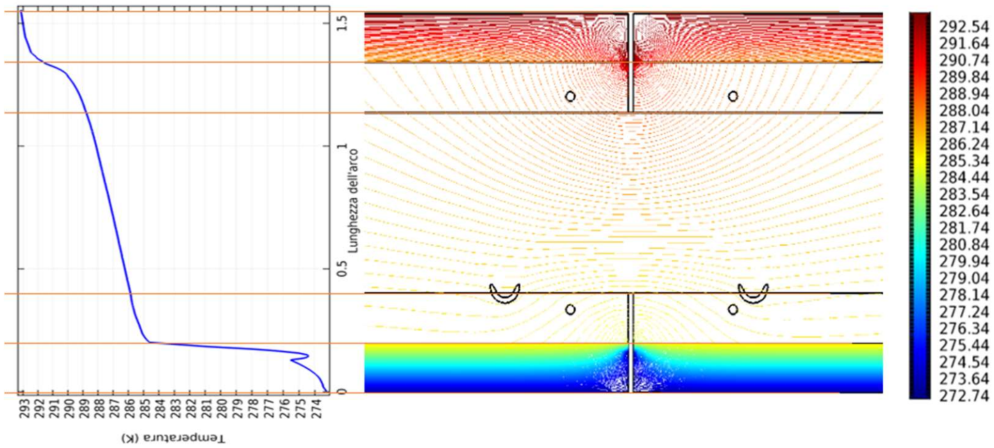

Figure 14. Temperature distribution (**left**) and isothermal lines on a representative xy plane (**right**) of the system with conventional joints.

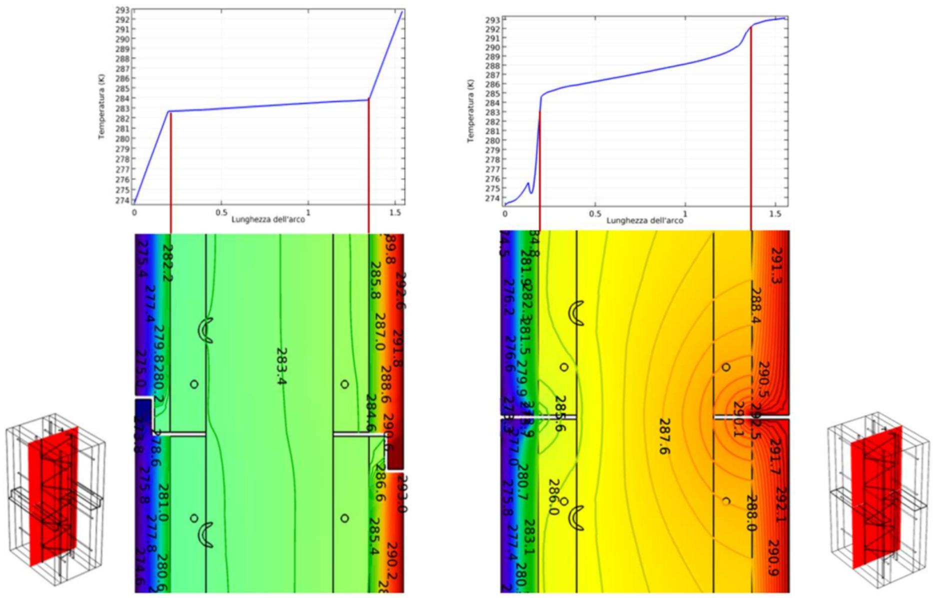

Figure 15. Comparison of the temperature maps and thermal isothermal lines on representative xz planes of the system with S-shaped (**left**) and conventional (**right**) joints.

It is worth mentioning that the behavior of the conventional joints is not significantly affected by the presence of finishings on the internal and external surfaces. In fact, assuming an internal 20 mm layer of gypsum–lime plaster and an external 1 mm layer of acrylic plaster, we can observe how the temperature trends are very similar to those relating to the solution without finishings. In this case, the temperature reductions from the indoor to the outdoor were found as follows: 0.2 K in the layer of gypsum–lime, 2.8 K in the EPS panel, 1.5 K in the RC panel, 2.5 K in the inner cavity, 1 K in the RC panel, 11.5 K in the EPS panel and 0.5 K in the layer of acrylic plaster (Figure 16). The comparison between the trends of the isothermal lines relative to the solutions without and with the finishing layers shows how they have the same trend and how said layers do not provide any significant contribution in terms of attenuation of the thermal bridge (Figure 17).

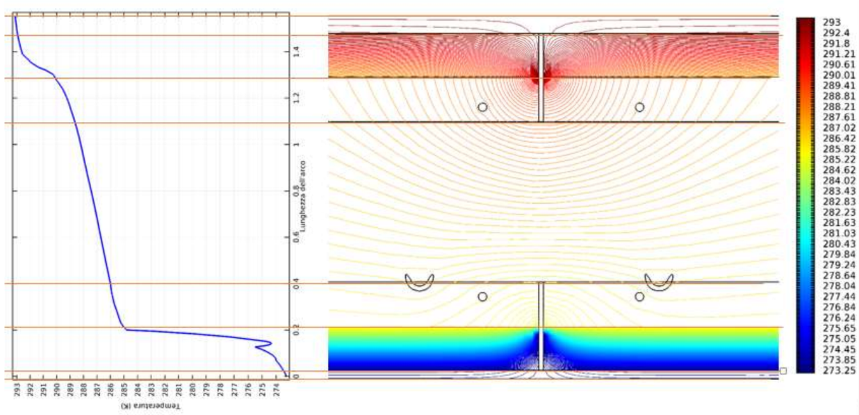

Figure 16. Temperature distribution (**left**) and isothermal lines on a representative xy plane (**right**) of the system with conventional joints and finishing layers.

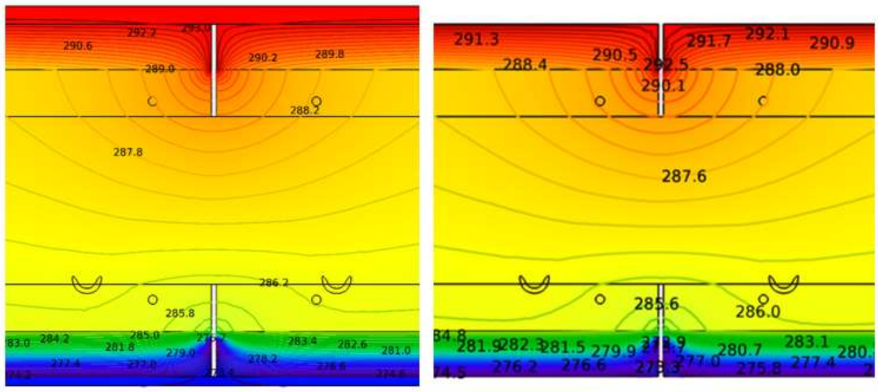

Figure 17. Comparison of the thermal isothermal lines on representative xz planes of the system with (**left**) and without (**right**) finishings.

5. Conclusions

The paper has proposed and validated the overall improvement of the energy performances of a patented precast EPS-RC double skin wall, addressing both the design of high-performing insulation solutions and the selection of sustainable materials, according to a life-cycle approach. To this end, some new formulations for the concrete mixtures were studied and tested, based on the partial or total replacement of the volume of sand aggregates with EPS granules, as discarded from the production process. The results showed that, depending on the mix design, a variety of conglomerates—lightweight or normal, structural or non-structural—might be produced that combine different levels of thermal insulation, mechanical resistance and reuse of tailings as secondary raw materials.

Furthermore, suitable horizontal and vertical joints with S-shaped profiles to connect the adjacent wall modules were designed and simulated in order to prevent constructional thermal bridges. The results showed that the proposed solutions are effective for the purpose, and confirmed that the wall system with an external EPS panel is not significantly affected by the presence of the inner reinforcement in terms of thermal anomalies on the outdoor surface. In conclusion, the research has provided reliable data for the feasible, effective and versatile application of the investigated building components, as well as contributing toward the optimization of prefabrication products and processes, as key actors in the path toward the energy efficiency and sustainability of new constructions and deep renovations.

Author Contributions: Conceptualization of the research: A.S. and F.F.; conceptualization of the paper: A.S. and M.D.F.; methodology: A.S. and M.D.F.; testing procedures: A.S.; software simulations:

A.S. and S.M.; discussion of results: A.S., M.D.F. and S.M.; validation: A.S., F.F. and M.D.F.; writing—original draft preparation: A.S. (Section 3.2) and M.D.F. (Sections 1, 2, 3.1 and 4); writing—review and editing: M.D.F.; supervision: F.F.; funding acquisition: F.F. All authors have read and agreed to the published version of the manuscript.

Funding: This research was partially funded by the Apulian Region (Italy) under the founding Framework POR PUGLIA FESR 2007–2013 Innonetwork.

Institutional Review Board Statement: Not applicable.

Informed Consent Statement: Not applicable.

Data Availability Statement: Not applicable.

Acknowledgments: The authors would like to acknowledge Ferramati International S.r.l. for supporting the production and testing of the component, and Alessandra Pierucci for collaborating in the manufacturing and testing of the specimens.

Conflicts of Interest: The authors declare no conflict of interest.

References

1. Cao, X.; Dai, X.; Liu, J. Building energy-consumption status worldwide and the state-of-the-art technologies for zero-energy buildings during the past decade. *Energy Build* **2016**, *128*, 198–213. [CrossRef]
2. Campagna, L.M.; Fiorito, F. On the Impact of Climate Change on Building Energy Consumptions: A Meta-Analysis. *Energies* **2022**, *15*, 354. [CrossRef]
3. Salvalai, G.; Sesana, M.M.; Iannaccone, G. Deep renovation of multi-storey multi-owner existing residential buildings: A pilot case study in Italy. *Energy Build* **2017**, *148*, 23–36. [CrossRef]
4. Motuzienė, V.; Rogoža, A.; Lapinskienė, V.; Vilutienė, T. Construction solutions for energy efficient single-family house based on its life cycle multi-criteria analysis: A case study. *J. Clean. Prod.* **2016**, *112*, 532–541. [CrossRef]
5. Salvalai, G.; Sesana, M.M.; Brutti, D.; Imperadori, M. Design and Performance Analysis of a Lightweight Flexible nZEB. *Sustainability* **2020**, *12*, 5986. [CrossRef]
6. Ibrahim, M.; Ibrahim, M. Estimating the sustainability returns of recycling construction waste from building projects. *Sustain. Cities Soc.* **2016**, *23*, 78–93. [CrossRef]
7. Kim, S.; Lee, D.-E.; Kim, Y.; Kim, S. Development and Application of Precast Concrete Double Wall System to Improve Productivity of Retaining Wall Construction. *Sustainability* **2020**, *12*, 3454. [CrossRef]
8. Navarro-Rubio, J.; Pineda, P.; García-Martínez, A. Sustainability, prefabrication and building optimization under different durability and re-using scenarios: Potential of dry precast structural connections. *Sustain. Cities Soc.* **2020**, *44*, 614–628. [CrossRef]
9. Zhang, J.; Long, Y.; Lv, S.; Xiang, Y. BIM-enabled Modular and industrialized Construction in China. *Procedia Eng.* **2016**, *145*, 1456–1461. [CrossRef]
10. Zhang, C.; Hu, M.; Laclau, B.; Garnesson, T.; Yang, X.; Li, C.; Tukker, A. Environmental life cycle costing at the early stage for supporting cost optimization of precast concrete panel for energy renovation of existing buildings. *J. Build. Eng.* **2021**, *35*, 102002. [CrossRef]
11. O'Hegarty, R.; Kinnane, O. Review of precast concrete sandwich panels and their innovations. *Constr Build Mater.* **2020**, *233*, 117145. [CrossRef]
12. O'Hegarty, R.; Kinnane, O.; Grimes, M.; Newell, J.; Clifford, M.; West, R. Development of thin precast concrete sandwich panels: Challenges and outcomes. *Constr Build Mater* **2021**, *267*, 120981. [CrossRef]
13. Graziani, L.; Quagliarini, E.; D'Orazio, M.; Lenci, S.; Scalbi, A. A More Sustainable Way for Producing RC Sandwich Panels On-Site and in Developing Countries. *Sustainability* **2017**, *9*, 472. [CrossRef]
14. Mugahed Amran, Y.H.; El-Zeadani, M.; Lee, Y.H.; Lee, Y.Y.; Murali, G.; Feduik, R. Design innovation, efficiency and applications of structural insulated panels: A review. *Structures* **2020**, *27*, 1358–1379. [CrossRef]
15. Expanded Polystyrene-Based Blocks for Formwork and Lightweight Blocks for Simple Formwork. Available online: https://evaluation.cstb.fr/en/certifications-products-services/product/entrevous-en-polystyrene-expanse-et-entrevous-legers-de-coffrage-simple/ (accessed on 21 December 2021).
16. KORE Insulating Concrete Formwork System. Available online: https://www.nsai.ie/images/uploads/certification-agrement/IAB080307.pdf (accessed on 21 December 2021).
17. Solomon, A.A.; Hemalatha, G. Characteristics of expanded polystyrene (EPS) and its impact on mechanical and thermal performance of insulated concrete form (ICF) system. *Structures* **2020**, *23*, 204–213. [CrossRef]
18. Amer-Yahia, C.; Majidzadeh, T. Inspection of Insulated Concrete Form walls with Ground Penetrating Radar. *Constr. Build Mater.* **2012**, *26*, 448–458. [CrossRef]
19. Sukontasukkul, P.; Sangpet, T.; Newlands, M.; Tangchirapat, W.; Limkatanyu, S.; Chindaprasirt, P. Thermal behaviour of concrete sandwich panels incorporating phase change material. *Adv. Build. Energy Res.* **2022**, *16*, 64–88. [CrossRef]

20. Marani, A.; Madhkhan, M. Thermal performance of concrete sandwich panels incorporating phase change materials: An experimental study. *J. Mater. Res. Technol.* **2021**, *12*, 760–775. [CrossRef]
21. Voellinger, T.; Bassi, A.; Heitel, M. Facilitating the incorporation of VIP into precast concrete sandwich panels. *Energy Build.* **2014**, *85*, 666–671. [CrossRef]
22. Da Gloria, M.Y.R.; Dias Toledo Filho, R. Innovative sandwich panels made of wood bio-concrete and sisal fiber reinforced cement composites. *Constr Build Mater.* **2021**, *272*, 121636. [CrossRef]
23. Šahmenko, G.; Šinka, M.; Namsone, E.; Korjakins, A.; Bajāre, D. Sustainable Wall Solutions Using Foam Concrete and Hemp Composites. *Environ. Clim. Technol.* **2021**, *25*, 917–930. [CrossRef]
24. Chippagiri, R.; Gavali, H.R.; Ralegaonkar, R.V.; Riley, M.; Shaw, A.; Bras, A. Application of Sustainable Prefabricated Wall Technology for Energy Efficient Social Housing. *Sustainability* **2021**, *13*, 1195. [CrossRef]
25. Šantek Bajto, J.; Štirmer, N.; Cerković, S.; Carević, I.; Kostanić Jurić, K. Pilot Scale Production of Precast Concrete Elements with Wood Biomass Ash. *Materials* **2021**, *14*, 6578. [CrossRef]
26. Rodriguez, C.; Miñano, I.; Parra, C.; Pujante, P.; Benito, F. Properties of Precast Concrete Using Food Industry-Filtered Recycled Diatoms. *Sustainability* **2021**, *13*, 3137. [CrossRef]
27. Dissanayake, D.M.K.W.; Jayasinghe, C.; Jayasinghe, M.T.R. A comparative embodied energy analysis of a house with recycled expanded polystyrene (EPS) based foam concrete wall panels. *Energy Build.* **2017**, *135*, 85–94. [CrossRef]
28. Fernando, P.L.N.; Jayasinghe, M.T.R.; Jayasinghe, C. Structural feasibility of Expanded Polystyrene (EPS) based lightweight concrete sandwich wall panels. *Constr Build Mater.* **2017**, *139*, 45–51. [CrossRef]
29. Awan, A.B.; Shaikh, F.U.A. Compressive behavior of precast concrete sandwich panels containing recycled tyre crumb rubber core. *Struct. Concr.* **2021**, *22*, 3602–3619. [CrossRef]
30. Lee, B.-J.; Pessiki, S. Thermal performance evaluation of precast concrete three-wythe sandwich wall panels. *Energy Build.* **2006**, *38*, 1006–1014. [CrossRef]
31. Zhai, X.; Wang, Y.; Wang, X. Thermal performance of precast concrete sandwich walls with a novel hybrid connector. *Energy Build.* **2018**, *166*, 109–121. [CrossRef]
32. Kim, Y.J.; Allard, A. Thermal response of precast concrete sandwich walls with various steel connectors for architectural buildings in cold regions. *Energy Build.* **2014**, *80*, 137–148. [CrossRef]
33. Scioti, A.; Pierucci, A.; De Fino, M.; Fatiguso, F. Pre-casting, recycle and performance efficiency for sustainable construction components. In Proceedings of the CIB World Building Congress 2019 "Constructing Smart Cities", Hong Kong, China, 17–21 June 2019.
34. Scioti, A. Pre-cast concrete walls: Techniques and technologies for performance optimization. *TEMA* **2015**, *1*, 83–88.
35. Wu, S.; Li, H.; Wang, X.; Li, R.; Tian, C.; Hou, Q. Seismic performance of a novel partial precast RC shear wall with reserved cast-in-place base and wall edges. *Soil Dyn.* **2022**, *152*, 107038. [CrossRef]
36. Jiang, J.; Luo, J.; Xue, W.; Hu, X.; Qin, D. Seismic performance of precast concrete double skin shear walls with different vertical connection types. *Eng. Struct.* **2021**, *245*, 112911. [CrossRef]
37. Lu, X.; Memari, A. Comparative Energy Analysis and Life-Cycle Assessment of Innovative Residential Wall Systems in Cold Regions. *Pract. Period. Struct.* **2019**, *24*, 04019015. [CrossRef]
38. Hachem-Vermette, C. Selected High-Performance Building Envelopes. In *Solar Buildings and Neighborhoods*; Green Energy and Technology; Springer: Berlin/Heidelberg, Germany, 2020; pp. 67–100.
39. Cruz, A.S.; Cunha, E.G. The impact of climate change on the thermal-energy performance of the SCIP and ICF wall systems for social housing in Brazil. *Indoor Built Environ.* **2021**. Available online: https://journals.sagepub.com/doi/abs/10.1177/1420326X211038047 (accessed on 1 January 2022). [CrossRef]
40. Nibhanupudi, P.; Rahul, G.B. Comparative study on use of precast framed structure and precast load bearing wall structure. *Mater. Today Proc.* **2020**, *33*, 537–542. [CrossRef]
41. Hilal, N.; Hamah Sor, N.; Faraj, R.H. Development of eco-efficient lightweight self-compacting concrete with high volume of recycled EPS waste materials. *Environ. Sci. Pollut. Res.* **2021**, *28*, 50028–50051. [CrossRef]
42. Mohammed, H.J.; Hussein, Y.G. Concrete Properties using Treated Recycled EPS. *IOP Conf. Ser. Earth Environ. Sci.* **2021**, *877*, 012028. [CrossRef]
43. Gopinathan, M.J.; Subramanian, K. High Performance and Efficiency of Joints in Precast Members. *Int. J. Eng. Sci. Technol.* **2013**, *5*, 4002–4009.
44. Lu, Z.; Wu, B.; Yang, S.; Hou, J.; Ji, Z.; Li, Y.; Huang, J.; Zhang, M. Experimental study on flexural behaviour of prefabricated concrete beams with double-grouted sleeves. *Eng. Struct.* **2021**, *248*, 113237. [CrossRef]
45. Gonçalves, M.; Simões, N.; Serra, C.; Flores-Colen, I.; Rottenbacher, K.; Flávia, A. Almeida, Study of the edge thermal bridging effect in vacuum insulation panels: Steady and unsteady-state approaches using numerical and experimental methods. *Energy Build.* **2022**, *258*, 111821. [CrossRef]
46. Gonçalves, M.; Simões, N.; Serra, C.; Flores-Colen, I. A review of the challenges posed by the use of vacuum panels in external insulation finishing systems. *Appl. Energy* **2020**, *257*, 2020. [CrossRef]
47. Song, J.H.; Lim, J.H.; Song, S.Y. Evaluation of alternatives for reducing thermal bridges in metal panel curtain wall systems. *Energy Build.* **2016**, *127*, 138–158. [CrossRef]
48. Sorensen, T.; Thomas, R.; Dorafshan, S.; Maguire, M. Thermal Bridging in Concrete Sandwich Walls. *Concr. Int.* **2018**, *40*, 45–49.

49. Martiradonna, S.; Fatiguso, F.; Lombillo, I. Thermal improvements of the existing reinforced concrete buildings by the precast concrete panel system. In Proceedings of the Colloqui.AT.e 2020—New Horizons for Sustainable Architecture, Catania, Italy, 10 January 2022.
50. Gencel, O.; del Coz Díaz, J.J.; Sutcu, M.; Kocyigit, F.; Rabanal, F.P.Á.; Alonso-Martínez, M.; Barrera, G.M. Thermal Performance Optimization of Lightweight Concrete/EPS Layered Composite Building Blocks. *Int. J. Thermophys.* **2021**, *42*, 52. [CrossRef]
51. UNI EN ISO 10456:2008. Building Materials and Products—Hygrothermal Properties—Tabulated Design Values and Procedures for Determining Declared and Design Thermal Values. Available online: http://store.uni.com/catalogo/uni-en-iso-10456-2008 (accessed on 12 November 2021).
52. UNI EN ISO 13788:2013. Hygrothermal Performance of Building Components and Building Elements—Internal Surface Temperature to Avoid Critical Surface Humidity and Interstitial Condensation—Calculation Methods. Available online: http://store.uni.com/catalogo/uni-en-iso-13788-2013 (accessed on 12 November 2021).
53. UNI EN 12667:2002. Thermal Performance of Building Materials and Products—Determination of Thermal Resistance by Means of Guarded Hot Plate and Heat Flow Meter Methods—Products of High and Medium Thermal Resistance. Available online: http://store.uni.com/catalogo/uni-en-12667-2002 (accessed on 12 November 2021).
54. ISO 12572:2016. Hygrothermal Performance of Building Materials and Products—Determination of Water Vapour Transmission Properties—Cup Method. Available online: http://store.uni.com/catalogo/iso-12572-2016 (accessed on 12 November 2021).
55. UNI EN 12390-2:2019. Testing Hardened Concrete—Part 2: Making and Curing Specimens for Strength Tests. Available online: http://store.uni.com/catalogo/uni-en-12390-2-2019 (accessed on 17 December 2021).
56. UNI EN 12390-3:2019. Testing Hardened Concrete—Part 3: Compressive Strength of Test Specimens. Available online: http://store.uni.com/catalogo/uni-en-12390-3-2019 (accessed on 17 December 2021).
57. UNI EN 12390-4:2019. Testing Hardened Concrete—Part 4: Compressive Strength—Specification for Testing Machines. Available online: http://store.uni.com/catalogo/uni-en-12390-4-2019 (accessed on 17 December 2021).
58. UNI EN 206:2021. Concrete—Specification, Performance, Production and Conformity. Available online: http://store.uni.com/catalogo/uni-en-206-2021 (accessed on 17 December 2021).
59. NTC2018. Italian Technical Normative for Construction. Available online: http://www.ingegneriasoft.com/pdf/Norme_Tecniche_Costruzioni_2018_NTC2018_NTC.pdf (accessed on 22 January 2022).
60. DPR n. 412, 26 August 1993. Regulation Laying Down Rules for the Design, Install Ation, Operation and Maintenance of the Thermal Systems of the Buildings for the Purpose of Containment of Energy Consumption. Available online: https://www.gazzettaufficiale.it/eli/id/1993/10/14/093G0451/sg (accessed on 22 January 2022). (In Italian)